IEEE Access
Multidisciplinary | Rapid Review | Open Access Journal

Received February 1, 2021, accepted February 12, 2021, date of publication February 22, 2021, date of current version March 4, 2021.

Digital Object Identifier 10.1109/ACCESS.2021.3061266

Vision-Based Traffic Conflict Detection Using Trajectory Learning and Prediction

ZONGYUAN SUN[1], YUREN CHEN[2], PIN WANG[3], (Member, IEEE), SHOUEN FANG[2], AND BOMING TANG[1]

[1]Department of Traffic and Transportation, Chongqing Jiaotong University, Chongqing 400074, China
[2]School of Transportation Engineering, Tongji University, Shanghai 201804, China
[3]California PATH, University of California at Berkeley, Berkeley, CA 94804, USA

Corresponding author: Zongyuan Sun (sunzy@cqjtu.edu.cn)

This work was supported in part by the National Key Research and Development Program of China under Grant 2018YFB1600200, and in part by the Natural Science Foundation of Chongqing, China, under Grant cstc2019jcyj-bshX0099.

ABSTRACT Although traffic conflict techniques have proven to be effective means for road safety analysis, they still suffer from incomplete conceptualization, observer subjectivity, and high data collection cost. To address these problems, video analysis has been increasingly applied to gain a better understanding of the behaviors of road users based on detailed motion data. However, the motion patterns underlying these data are rarely extracted to study the safety of their interactions. This article presents a vision-based method of traffic conflict detection through learning motion patterns from trajectories, for which an original algorithm was established through clustering and subsequent modeling. Using the extracted path and velocity information, we clustered trajectories hierarchically by applying an improved fuzzy K-means algorithm with a modified Hausdorff distance. Each obtained cluster was taken as a labeled set to determine the structure and train the parameters of a hidden Markov model (HMM) that encoded the spatiotemporal characteristics of the trajectories as motion patterns. Based on the targeted trajectory predictions by the learned HMMs following the conflict development, a probabilistic model was developed to estimate the collision likelihood between vehicles to identify traffic conflicts. The experimental results obtained using actual traffic videos demonstrated the applicability of the algorithms for learning motion patterns and the feasibility of the approach for traffic conflict detection. The predicted trajectories were sufficiently accurate to calculate the collision probability, which was qualified as an indicator for measuring the conflict severity. These findings will have important implications for effective improvements in active road safety.

INDEX TERMS Collision estimation, hidden Markov model (HMM), motion pattern, traffic conflict detection, trajectory learning, video analysis.

I. INTRODUCTION

Road safety analysis is traditionally conducted based on traffic crash data. However, it is well recognized that such data suffer from quantity and quality problems. Additionally, because analysis can only be applied following the accumulation of sufficient crash data, it generally has to be conducted in a passive manner. These shortcomings have led to the study of traffic conflict techniques (TCTs) in an attempt to establish active methods accordingly [1]–[3]. Traffic conflict analysis involves the assessment of inter-vehicle interactions that are broadly similar to collisions and therefore has the advantages of large sample sizes, short analysis time intervals, high reliability, etc. Traffic conflicts are conventionally identified by groups of trained observers who analyze the interactions between two or more vehicles approaching each other. In such cases, if either one of the vehicles does not change its motion, the vehicles will collide, and the situation is defined as a traffic conflict [4]. However, owing to imperfect conceptualization, the high cost of training observers, data availability problems, and the subjectivity and questionable reliability of the observers, TCTs have developed relatively slowly over time.

The recent rapid growth of computer vision and machine learning, along with the powerful abilities of these techniques to collect and analyze motion vision information, has made it possible to address the problems that have restricted the development of TCTs. Furthermore, as noted in the Highway

The associate editor coordinating the review of this manuscript and approving it for publication was Alessia Saggese.

Safety Manual [5], it is necessary to replace conventional statistical models with microscopic models that can more clearly reflect the mechanisms of collisions in future road safety studies. Numerous researchers have already applied detailed microscopic vehicle motion data obtained via video analysis to detect traffic conflicts. However, they differ significantly in the manner in which they have addressed the core problem of vehicle trajectory learning and prediction. Some researchers [6]–[12] have proposed a range of metrics that can describe the degree of interaction between vehicles in detail (e.g., time-to-collision (*TTC*), post-encroachment time, time advantage, and time gap). Nonetheless, these metrics are only calculated using direct approaches in which the vehicle trajectories are extrapolated by constant velocity and direction. In a structured roadway scenario, vehicles actually neither move at random, nor do they move at constant velocities. Instead, they follow underlying motion patterns that correspond to driver intent, which can be learned and used to predict future motions. Correspondingly, other researchers [13]–[17] have sought to detect traffic conflict using the estimated collision possibility, *TTC*, and other indicators via trajectory learning.

Trajectory learning algorithms for predicting the motion of road users can be classified into two primary categories: discrete state-space model-based and neural network-based approaches. The former algorithms generally cluster trajectories and learn the clustering results by applying discrete state-space models to obtain the vehicle motion patterns closest to the trajectory prototypes. The clustering algorithms used for this purpose include K-means clustering [18], [19], hierarchical clustering [20], [21], graph cutting [22], pairwise clustering [23], [24], spectral clustering [25], [26], and expectation-maximization-based clustering [27]. Regarding model selection, a trajectory cluster is commonly developed as a path model [19]–[23], [26], [28], which is characterized by an average central spline with two lateral extremal boundaries that define the variations of the trajectories within the cluster. The width of the path is determined using a deterministic or probabilistic method. Other existing models [18], [27], [29]–[31] are primarily based on hidden Markov models (HMMs) in which space and time are regarded as discrete variables and spatiotemporal trajectory patterns are learned using several discrete states.

Neural networks are probably the most widely used alternatives to discrete state-space models. Johnson and Hogg [32] first applied a multilayer self-organizing network to learn object trajectory patterns. In their method, a set of flow vectors constituting the prototype trajectories was input into the network and quantized using two competitive learning networks connected by a layer of leaky neurons: one to learn the distribution of flow vectors and another to learn the distribution of trajectories. A similar neural network was developed by Sumpter and Bulpitt [33], who added a feedback loop to the network to improve the motion prediction accuracy. Hu *et al.* [34] further improved on this work by designing a hierarchical self-organizing neural network in which the side neurons in the output layer were linked to form an internal net that replaced the leaky network layer. Subsequently, they [13] developed a more concise self-organizing neural network for learning activity patterns. Although research on such methods seems to have stalled in recent years, lately some researchers have attempted to apply recurrent neural networks with long short-term memory model [35], [36] or multilayer perceptrons [37] to strengthen trajectory learning. A different framework proposed by Stauffer and Grimson [38] involved the construction of a co-occurrence matrix for trajectories in each motion pattern, which are learned by applying a hierarchical classification to the matrix. Other researchers [39], [40] have simplified traffic conflict detection into two-class problems that can be solved without trajectory prediction using supervised learning and the recognition of conflict trajectories.

Among the solutions for traffic conflict detection through video analysis techniques, the most promising ones are those that rely on trajectory learning algorithms rather than direct extrapolation to predict trajectories in a more realistic and accurate fashion [41], [42]. Unlike neural network-based methods, discrete state-space models can learn the variable lengths of trajectories as sequence data in a natural manner [30]. However, the existing models rarely consider both the space and time uncertainties of trajectories, with majority of them focusing on the discrete state analysis of space rather than time. This deficiency inevitably limits the applicability and flexibility of such models and hinders their ability to perform thorough statistical analyses of motion patterns, particularly in terms of vehicle-speed prediction. More seriously, some models rely on destructive trajectory pre-processing techniques, such as resampling via linear interpolation [27], [28], [43] or padding with default values [13], [19], to normalize the trajectory lengths. These operations lead to the distortion of spatial information and loss of temporal information. Consequently, the trajectory predictions made by such models are even more difficult to conduct at the time-discrete state level than other discrete state-space models.

The objective of this study is to develop a methodology for the visual detection of traffic conflict through the learning of vehicle trajectories to explore fully their usefulness in characterizing motion patterns. In general, trajectory learning is best performed automatically in an unsupervised manner to construct the motion pattern of an object in a given scenario [44]. However, if the complex and variable vehicle trajectories are clustered in advance and the results are used to guide trajectory modeling, the original *blind* unsupervised work will be transformed into a supervised one, thereby improving the efficiency and accuracy of learning. With this aspect in mind, we present an original cluster-and-model method for trajectory learning. Without the need for distorted pre-processing of trajectories, an improved fuzzy K-means algorithm with a modified Hausdorff distance is proposed to cluster them hierarchically based on their implied paths and velocity characteristics. Then, the HMM is employed to model comprehensively the spatiotemporal uncertainties of trajectories in each obtained cluster, the mixture of which

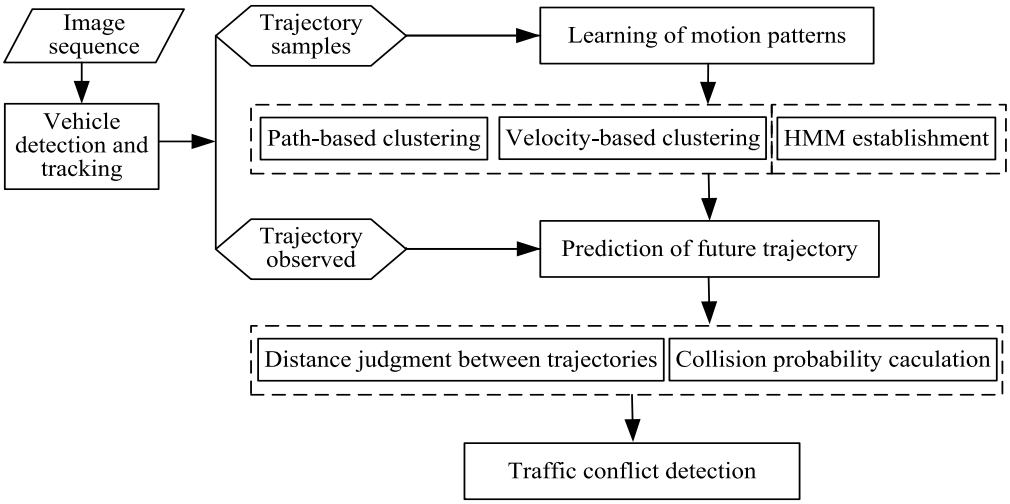

FIGURE 1. Overview of the proposed traffic conflict detection approach.

represents all underlying motion patterns. Based on the characteristics of conflict development, a more targeted algorithm for the prediction of trajectory covering varying velocities than the usual absolutely statistical distribution of paths with constant velocity was established and merged into a probability model to estimate collisions for the detection of traffic conflicts. The results of this study can be used to exploit trajectories fully for effective detection of traffic conflicts and provide insights into the improvement of the visual analysis and understanding of vehicle motion behavior.

II. METHODOLOGY

For any given road environment, the proposed method acquires raw trajectories by detecting and tracking vehicles across multiple frames extracted from video. After resampling n times at a larger time interval (once every Δt frames), a sample vehicle trajectory can be represented by the set F_l comprising n flow vectors $F_l = \{f_1, f_2, \ldots, f_t, \ldots, f_{n-1}, f_n\}$, where $f_t = \left(x_t, y_t, \delta_{x_t}, \delta_{y_t}\right)$. In each vector f_t, $p_t = (x_t, y_t)$ and $V_t = \left(\delta_{x_t}, \delta_{y_t}\right)$ respectively represent the world coordinates of the centroid and velocity of the vehicle at the t-th sampling interval. The collection of individual F is then used to compile a set of sample trajectories $\Omega = \{F_1, F_2, \ldots, F_l, \ldots, F_J\}$, where J denotes the number of sample trajectories and F_l is the l-th trajectory. The proposed approach consists of three components: the learning of motion patterns (i.e., hierarchical clustering of trajectories and training HMMs with trajectories in the corresponding cluster); trajectory prediction; and traffic conflict detection (as shown in Figure 1).

A. HIERARCHICAL TRAJECTORY CLUSTERING WITH IMPROVED FUZZY K-MEANS ALGORITHM

A natural approach to identifying potential motion patterns involves applying a clustering algorithm to assign similar trajectories to the same group [45]. If there are numerous highly diverse samples, the direct implementation of trajectory clustering will involve a heavy computational load for calculating the distance between trajectories, resulting in significantly slower the process. Considering the purpose of clustering and the need for efficiency, a hierarchical clustering algorithm for trajectories based on spatiotemporal information of vehicle motion can be applied instead. The proposed method first applies path clustering according to the spatial position of each trajectory. It then clusters the results further according to the vehicle velocity to produce a set of trajectory clusters with spatial and temporal differentiation. As there will inevitably be an overlap between some trajectories in addition to the presence of abnormal trajectories in the samples, hard classification results produced by the common clustering method will inevitably deviate from the actual situation. Although the fuzzy K-means algorithm can address the overlapping trajectory problem, it is, in several respects, restricted in terms of practical use [19]. By contrast, the improved fuzzy K-means algorithm can not only address the existence of wild values, but is also insensitive to pre-defined numbers of clusters, owing to its relaxed membership conditions. The enhanced robustness and applicability of the improved fuzzy K-means make it quite suitable for performing clustering at each layer.

1) PATH-BASED CLUSTERING

A path is defined as a geometric curve described by the coordinates of each point on a trajectory and reflects the most important position and curve shape characteristics of the trajectory. The proposed method initially clusters trajectories in terms of their path information. For a set of sample trajectories Ω, the corresponding set of intermediate trajectories for path-based clustering can be represented as $\Omega' = \left\{F'_1, F'_2, \ldots, F'_l, \ldots, F'_J\right\}$, where $F'_l = \left\{f'_1, f'_2, \ldots, f'_t, \ldots, f'_n\right\}$. To improve the efficiency

of clustering, only the coordinates of points $f_t' = (x_t, y_t)$ $(t = 1, 2,\ldots,n)$ on each trajectory of each set F_l' are retained, as they can adequately reflect the path characteristics.

The improved fuzzy K-means-based algorithm is used to create a mapping between the intermediate trajectories and their cluster centroids, which retain the spatial distribution of the trajectories. To compare the trajectories, a reliable distance metric must be first introduced. In this case, the Hausdorff distance [22], [25] was preliminarily selected rather than metrics such as the Euclidean distance, dynamic time warping, and longest common subsequence similarity, because it is more suitable for measuring distances between point sets (e.g., trajectories) [44]. As the measurement error of the traditional Hausdorff distance increases with the difference in lengths between trajectories, the modified one [46], which specifically addresses this problem, is used to measure the distance between trajectories F_i' and F_j':

$$D_H\left(F_i', F_j'\right) = \min_{1 \le i,j \le J}\left(D_h\left(F_i', F_j'\right), \quad D_h\left(F_j', F_i'\right)\right) \tag{1}$$

with

$$\begin{cases} D_h\left(F_i', F_j'\right) = \max\limits_{f_{i,k}'}\left(\min\limits_{f_{j,l}'} d_E\left(f_{i,k}', f_{j,l}'\right)\right), & \forall k, l \\ D_h\left(F_j', F_i'\right) = \max\limits_{f_{j,l}}\left(\min\limits_{f_{i,k}} d_E\left(f_{j,l}', f_{i,k}'\right)\right), & \forall l, k \end{cases} \tag{2}$$

where $d_E\left(f_{i,k}', f_{j,l}'\right)$ is the Euclidean distance between the k-th and l-th characteristic vectors $f_{i,k}'$ and $f_{j,l}'$, respectively. The reasonable clustering results should be separated by a certain distance, and the farther the better. Because the improved fuzzy K-means-based algorithm is sensitive to the initial values of cluster centroids, the K-means ++ algorithm is employed to initialize them to obtain satisfactory results. After a sample is chosen as the first cluster centroid θ_1 randomly, the following c–1 centroids are determined by roulette wheel selection according to the probability that each sample is selected as the next one $P(F_i)$, which is calculated as follows:

$$P(F_i) = \frac{D_{F_i}^2}{\sum_{i=1}^{n} D_{F_i}^2} \tag{3}$$

where $D(F_i)$ is the shortest modified Hausdorff distance from a data sample to the closest center already determined. Subsequently, based on the modified Hausdorff distance, the fuzzy membership $\varphi_{cl}(t)$ of each sample F_l' to each cluster centroid θ_c is calculated as follows:

$$\varphi_{cl}(t) = \frac{J/D_H^2\left(F_l', \theta_c\right)}{\sum_{c=1}^{K}\sum_{l=1}^{J}\left(1/D_H^2\left(F_l', \theta_c\right)\right)}. \tag{4}$$

The cluster centroid vectors are then adjusted iteratively using

$$\theta_c\,(t+1) = \frac{\sum_{l=1}^{J} \varphi_{cl}^2\,(t)\,F_l'}{\sum_{l=1}^{J} \varphi_{cl}^2\,(t)} \tag{5}$$

until the following constraint condition is satisfied:

$$\max_{1 \le c \le K}\left[D_H\left(\theta_c(t+1), \theta_c(t)\right)\right] < \varepsilon. \tag{6}$$

2) VELOCITY-BASED CLUSTERING

Although the subsets of Ω_c $(c = 1, 2,\ldots, K)$ can represent different motion paths of vehicles, they are not sufficient to characterize the motion patterns of vehicles, because in actual scenarios, vehicles can stop, worm, or rush along a given path. To fulfill the clustering goal of learning and predicting the motion patterns of vehicles, it is necessary to cluster trajectories further within the subsets of Ω_c based on their speed information. Therefore, the modified Hausdorff distance can be extended to measure the temporal similarities between trajectories, whose original flow vector f already contain speed information. In this regard, a clustering algorithm based on the improved fuzzy K-means algorithm performs identically to path-based clustering. Notably, because the scale of a subset of Ω_c is considerably smaller than that of the overall set Ω, the computational complexity of the subset clustering process is much lower than that of direct clustering. When this velocity-based clustering process is completed, each Ω_c is further divided into different subsets, and the overall set of sample trajectories is correspondingly clustered into Z sets of trajectories:

$$\begin{cases} \Omega = \left\{\left\{F_{1,1}, \ldots, F_{1,M_1}\right\}, \ldots, \right. \\ \qquad \left.\left\{F_{r,1}, \ldots, F_{r,M_r}\right\}, \ldots, \left\{F_{Z,1}, \ldots, F_{Z,M_Z}\right\}\right\} \\ \sum_{r=1}^{Z} M_r = J \end{cases} \tag{7}$$

where M_r is the number of original trajectories in the r-th trajectory subset Ω_r.

B. LEARNING AND PREDICTING TRAJECTORIES USING HMMS

Clustering can only be used for inferencing after establishing an appropriate representation model. The discrete nature of trajectories makes discrete-state models (e.g., HMM) quite suitable for the approximate analysis of continuous motion [18], [19], [31]. HMMs can not only flexibly reflect the uncertainty in the positions through which a vehicle passes, but also describe the time dependencies between successive points. Through training, all trajectory samples can be mapped to hidden state parameters and state transition matrices of HMMs so that clustering can occur in a parameter space. To enable vehicle motion prediction, the trajectory clusters acquired using the approach described in Section II-A are

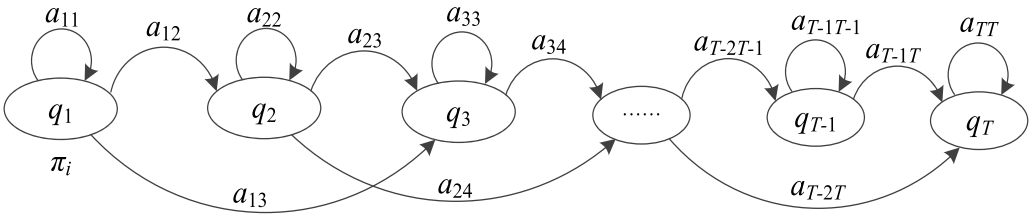

FIGURE 2. Left-to-right HMM for trajectories.

utilized as the basis for learning the HMMs with the probability distribution of the HMMs representing different motion patterns encoded by the number distribution of the trajectories belonging to the corresponding clusters.

1) HMM-BASED LEARNING ALGORITHM

a: HMM NOTATION AND STRUCTURE

An HMM is a random state machine [47], [48] that essentially consists of a two-layer system model in which a hidden first-order Markov process produces a visible observation sequence with a certain probability. The first layer describes the unobservable homogeneous Markov chain process according to the state transition matrix, whereas the second layer represents the random mechanism between the observed variables and the state. HMMs can effectively model sequences with complex spatiotemporal changes, varying length and noise characteristics without changing their time-order characteristics [49], [50]. For a detailed overview of HMMs, readers are directed to [48]. To define the HMMs used under the proposed method, we apply the following notations. The complete specification of a first-order HMM with N states $\{S_1, S_2, \ldots, S_N\}$ and a Gaussian observation density function for each state are formally given by the following probabilistic parameters:

1) The prior state probability distribution $\pi = \{\pi_i\}$, where $\pi_i = P(q_1 = S_i)$ and $\sum_{i=1}^{N} \pi_i = 1, \quad 1 \le i \le N$;
2) The state transition probability distribution $A = \{a_{i,j}\}$, where $a_{i,j} = P\left(\left[q_t = S_j\right] | [q_{t-1} = S_i]\right)$ and $\sum_{j=1}^{N} a_{i,j} = 1$, $1 \le i, j \le N$;
3) The observation probability density $B = \{b_j(o_t)\}$, where $b_j(o_t) = P\left([O_t = o_t] \left| \left[q_t = S_j\right]\right.\right) = N\left(o_t, \mu_j, \sum_j\right)$ for $1 \le j \le N$, where μ_j and $\sum_j$ are the mean and covariance, respectively, of the Gaussian of state S_j and o_t and q_t are the observation and state variable, respectively, at time t.

The full set of parameters describing the HMM is commonly denoted as $\lambda = (\pi, A, B)$. The essential precondition for ensuring the acquisition of reliable HMM is that the HMM structure must be properly determined before the trajectories can be learned. To reflect the transfer characteristics of vehicle trajectory dots, we adopt a structure in which the states move from left to right in one direction, as depicted in Figure 2. A vehicle can remain in a given state for a short time or proceed in continuous or jumping modes. Although trajectories are characterized more clearly when the number of HMM states is increased, increasing the number of states will increase the model size. Hence, the number of states was determined by the complexity of the trajectory samples and computational limitations in this study.

b: LEARNING THE PARAMETERS

Parameter learning occurs after the structure of the HMM has been determined. Intrinsically, this task can be considered a maximum likelihood problem in which the trajectory samples belonging to a cluster are used to optimize the HMM parameters so that they match the samples with maximum probability. Although the Baum–Welch formulas do not yield a global optimal solution, the HMM learning algorithm still mainly uses them to calculate parameters recursively to guarantee convergence to a local optimum. Using trajectory F as an observation sequence O, we can re-express the clustering of Ω_r in (7) as $\left\{O^1, O^2, \ldots, O^{M_r}\right\}$, where $O^l = \left\{o_1^l, o_2^l, \ldots, o_{T_l}^l\right\} = F_l$, $1 \le l \le M_r$ and $o_t = f_t$, $1 \le t \le T_l$. If we denote the maximum length of all trajectories in cluster Ω_r as L_r and the sampling distance as Δ, then the total number of states in the HMM is given by $E_r = \lceil L_r/\Delta \rceil$. Each set of successive points within the length range of Δ can then be considered as observable signals emitted by the corresponding state, and the transfer characteristics between them can be captured by the state transition matrix. According to the maximum likelihood principle, the trajectories in set Ω_r can eventually be mapped to the set of HMM parameters $\lambda = (\pi, A, B)$ using the likelihoods of each state and transition belonging to the optimal HMM as weights to update it as the following steps.

1) Initialize the state prior probabilities π and transition matrix A.
2) Input all trajectories $O^l = \left\{o_1^l, o_2^l, \ldots, o_{T_l}^l\right\}$, $1 \le l \le M_r$.
3) For every time t in O^l, compute the forward and backward probabilities:

$$\alpha_t^l(i) = P\left(o_1^l, o_2^l, \ldots, o_t^l, q_t = s_i \,|\lambda\right) \tag{8}$$

$$\beta_t^l(i) = P\left(o_{t+1}^l, o_{t+2}^l, \ldots, o_{T_l}^l \,|q_t = s_i\,, \lambda\right). \tag{9}$$

4) Calculate the probabilities of being in state S_i at time t and S_j at time $t+1$ ($\xi_t^l(i,j)$) and of being in S_i at time t ($\gamma_t^l(i)$), as follows:

$$\xi_t^l(i,j) = P\left(q_t = S_i, q_{t+1} = S_j \middle| O^l, \lambda\right) \tag{10}$$

$$\gamma_t^l(i) = \sum_{j=1}^{N} \xi_t^l(i,j) = P\left(q_t = S_i \middle| O^l, \lambda\right). \tag{11}$$

5) For each discrete state S_i, re-estimate the state prior $\hat{\pi}_i$, mean $\hat{\mu}_i$, and covariance $\hat{\Sigma}_i$ of the Gaussian as follows:

$$\hat{\pi}_i = \frac{1}{M_r} \sum_{l=1}^{M_r} \gamma_1^l(i) \tag{12}$$

$$\hat{\mu}_i = \frac{\sum_{l=1}^{M_r} \sum_{t=1}^{T_l} \gamma_t^l(i) o_t^l}{\sum_{l=1}^{M_r} \sum_{t=1}^{T_l} \gamma_t^l(i)} \tag{13}$$

$$\hat{\Sigma}_i = \frac{\sum_{l=1}^{M_r} \sum_{t=1}^{T_l} \gamma_t^l(i)(o_t^l - \mu_i)(o_t^l - \mu_i)^T}{\sum_{l=1}^{M_r} \sum_{t=1}^{T_l} \gamma_t^l(i)}. \tag{14}$$

6) Adjust the transition probability in A as follows:

$$\hat{a}_{ij} = \frac{\sum_{l=1}^{M_r} \sum_{t=2}^{T_l} \xi_{t-1}^l(i,j)}{\sum_{l=1}^{M_r} \sum_{t=2}^{T_l} \gamma_{t-1}^l(i)}. \tag{15}$$

7) Determine whether the convergence condition of the HMM is met, as follows:

$$|\log P(\Omega_r | \lambda_{t+1}) - \log P(\Omega_r | \lambda_t)| < \eta, \tag{16}$$

where

$$\begin{cases} P(\Omega_r | \lambda_{t+1}) = \prod_{l=1}^{M_r} P\left(O^l | \lambda_{t+1}\right) \\ P(\Omega_r | \lambda_t) = \prod_{l=1}^{M_r} P\left(O^l | \lambda_t\right) \end{cases}. \tag{17}$$

If the convergence condition is true, then the learning procedure terminates; otherwise, return to Step 2 for the next learning iteration.

2) TRAJECTORY PREDICTION

The trajectory covering the velocity of a vehicle can be predicted by utilizing the HMMs learned using the process described in Section II-B1. For a time-varying trajectory $O = \{o_1, o_2, \ldots, o_t\}$, this prediction is performed as follows.

For a new observation, the current belief state for the vehicle is calculated using

$$P(q_t | o_t) = \frac{1}{G} P(o_t | q_t) \sum_{q_{t-1}} \left[P(q_t | q_{t-1}) P(q_{t-1} | o_{t-1})\right] \tag{18}$$

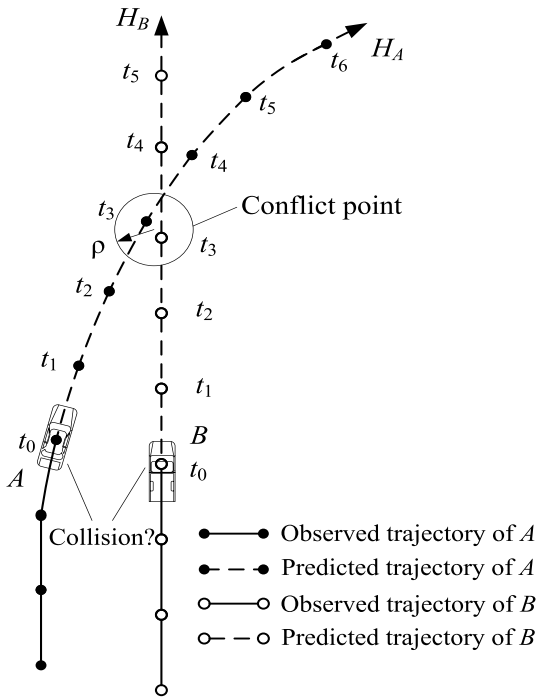

FIGURE 3. Prediction of collision between vehicles.

where G is the normalizing variable. By extrapolating this belief state R time steps into the future, a prediction can be made using the following recursive equation:

$$P(q_{t+R} | o_t) = \sum_{q_{t-1}} \left[P(q_{t+R} | q_{t+R-1}) P(q_{t+R-1} | o_t)\right]. \tag{19}$$

The development of a traffic conflict between vehicles generally undergoes four distinct stages: formation, exacerbation, mitigation, and elimination [14], [51]. In general, the severity of a conflict between vehicles entering a monitoring area increases over time. During this process, the movement trends of the respective vehicles become gradually clearer as the observed partial trajectory length increases, eventually enabling reliable motion prediction. As only severe conflicts are closely related to road safety [7], [52], [53], by utilizing the state distribution of vehicles at different times estimated using (19), the probability weighted mean of each state calculated with (20) is taken as the predicted trajectory of the vehicle:

$$\phi_{(t+R)} = \sum_{i=1}^{N} P(q_{t+R} = s_i | o_t) \mu_i. \tag{20}$$

C. DETECTING TRAFFIC CONFLICTS

After the trajectories of two vehicles in an interaction have been predicted, it is possible to infer whether they will collide at a future time. Assuming that the trajectories of vehicles A and B (H_A and H_B, respectively, in Figure 3) have been

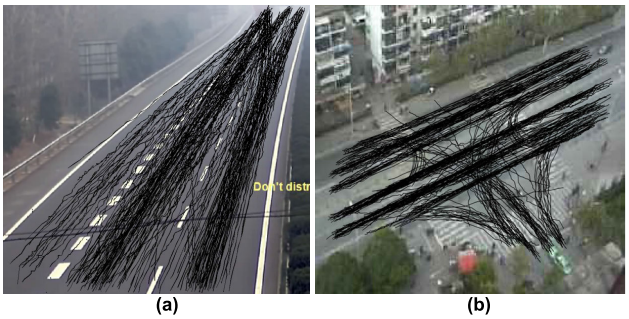

FIGURE 4. Two sets of trajectory samples in real test scenes. (a) freeway entrance. (b) urban road T-intersection.

predicted R time steps ahead, then, if from the current time t to $t+R$, the distance between H_A and H_B falls below the safety distance threshold ρ once or multiple times, it is estimated that the vehicles will collide at the first *TTC*. Although this deterministic analysis can predict whether the vehicles will collide, it does not consider the differences in terms of driver risk control abilities under different *TTCs*. In fact, as the *TTC* increases, it is more likely that one or both drivers will be able to adjust the motions of their vehicles and finally avoid a collision. Therefore, following [13, eq. (26)], we can estimate the collision probability for vehicles A and B at time t as

$$P_t\left(H_A, H_B\right) = \exp^{-\frac{TTC^2}{2\sigma^2}} \in [0, 1], \tag{21}$$

where σ is a normalizing factor that is equal to a perception and brake reaction time of 1.5 s [54]. After the collision probabilities of all interactions have been calculated, all traffic conflicts can be detected by setting a filter threshold on the conflict severity indicator.

III. RESULTS AND DISCUSSION

The proposed traffic conflict detection scheme algorithms were implemented using the Intel OpenCV library on a VS 2010 platform. Experiments were conducted based on several sets of video data obtained at different traffic scenes. Two typical results acquired at a freeway entrance and an urban road T-intersection were chosen to analyze the performance of our algorithms. Over the course of the 30-min-long video recording, 352 and 1095 vehicles passed through the entrance and T-intersection, respectively. A background differencing and blob-tracking system based on [55] was used to collect the raw vehicle trajectories. To acquire sample trajectories, the raw trajectories were first smoothed with an average moving filter and then validated in terms of minimum length and speed. Figure 4 illustrates the obtained trajectory sets of the freeway entrance and intersection, containing 405 and 1264 trajectories, respectively. The number of trajectories is slightly higher than the number of vehicles, because tracking failure caused some of the trajectories to split.

A. LEARNING HMMS

The sample trajectories were first clustered hierarchically using the improved fuzzy K-means algorithm described in Section II-A. Then, to determine the effectiveness of the improved algorithm, the clustering results were quantitatively compared with those of two other un-improved algorithms, which were based on the general K-means and fuzzy K-means algorithm [19], respectively, by the Tightness and Separation Criterion (*TSC*). Table 1 shows the *TSCs* of the clusters for the test scenes obtained by the algorithms with different initial cluster centroids and convergence conditions. As can be seen in the table, the improved algorithm was less affected by the initial cluster centroids and achieved much lower values of *TSC* than the un-improved ones. This finding indicates that our approach can cluster trajectories better than the other two algorithms. After modeling the clusters, the structures of the HMMs for the freeway entrance and T-intersection were acquired, as shown in Figure 5. During the learning process, the related parameters were tested by trial and error and finally set to $\varepsilon = 0.01$, $\Delta = 1.0$ m, and $\eta = 1 \times 10^{-4}$. Although, as stated in [14], it is generally difficult to evaluate unsupervised work, such as trajectory learning, the established structures appear to provide a satisfactory division of the trajectories reflecting their spatial distribution by visual judgment. In addition, the identified vehicle motion patterns are consistent with the intentions of drivers to move on, into, or out of the freeway at the entrance and T-intersection.

TABLE 1. *TSCs* of clusters obtained by different algorithms.

Convergence condition η	K-means		Fuzzy K-means		Improved fuzzy K-means	
	Entrance	Intersection	Entrance	Intersection	Entrance	Intersection
0.0001	1.4272	1.3852	0.5311	0.5230	0.3197	0.2698
	1.3503	1.1998	0.5179	0.5070	0.3152	0.2527
	1. 1106	0.9121	0.5004	0.4996	0.2911	0.2493
0.001	1.5218	1.4757	0.5796	0.5696	0.3298	0.2698
	1.2134	1.2817	0.5571	0.5257	0.3102	0.2569
	1.1314	1.0265	0.5180	0.5100	0.3013	0.2495
0.01	1.9806	1.9345	0.6413	0.6109	0.3262	0.2752
	1.7637	1.6831	0.6158	0.5541	0.3250	0.2608
	1.6519	1.5925	0.5710	0.5402	0.3115	0.2596

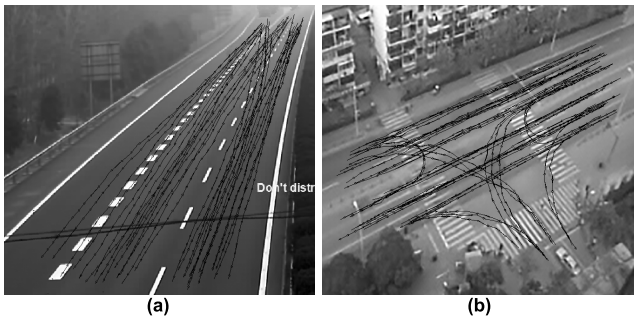

FIGURE 5. HMM structures learned in test scenes. (a) freeway entrance. (b) urban road T-intersection.

B. TRAJECTORY PREDICTION AND ACCURACY EVALUATION

The learned HMMs were validated further by testing their performances in trajectory estimation. Two typical examples of this process are shown in Figure 6, which illustrates how

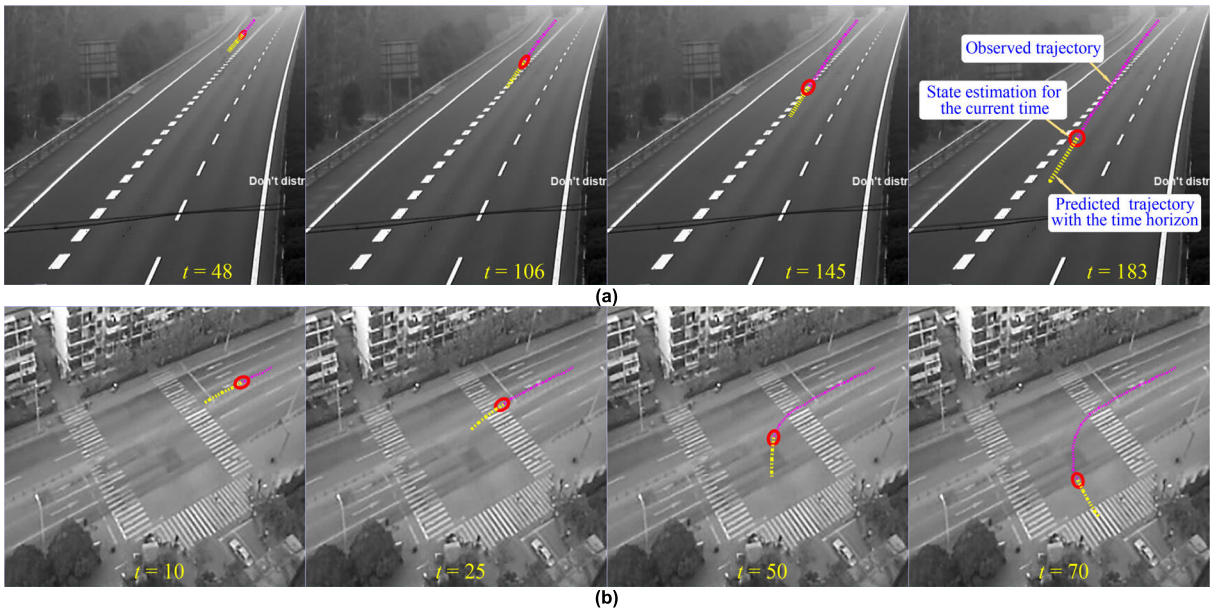

FIGURE 6. Two examples of trajectory prediction for a vehicle moving in the scenes. (a) freeway entrance sequence. (b) urban road T-intersection sequence.

the prediction method works within the prediction time range for time steps R from 1 to 15. The predicted trajectories for the two vehicles show that they will initially most likely move ahead in a straight line along the current lane and then tend to turn left, which became more evident as the motion progressed. Furthermore, the consistency presented between the observed trajectory and predicted trajectory qualitatively demonstrates the validity of the algorithms for predicting trajectories.

In addition to the aforementioned qualitative analysis, the mean estimation error was calculated to measure the accuracy of the trajectory prediction based on two additional test datasets differing from the learning samples and comprising 40 and 50 trajectories collected at the entrance and T-intersection, respectively. In this case, the mean estimation error was defined as the distance between the predicted point for the time horizon R and its corresponding position on the actual trajectory o_{t+R}:

$$E_{(R)} = \frac{1}{W}\sum_{l=1}^{W}\frac{1}{T_l - R}\sum_{t=1}^{T_l-R}\left\| o_{t+R}^{l} - \sum_{i=1}^{N} P\left(q_{t+R} = s_i \left| o_t^l \right.\right)\mu_i \right\|^{1/2} \quad (22)$$

where W is the number of test trajectories.

To measure the trajectory prediction performance more accurately, two other technologies using a fuzzy K-means (FKM) clustering [19] and the Expectation-Maximization (EM) algorithm [23] were implemented, and their prediction results were compared with those of our approach based on the improved fuzzy K-means (IFKM) clustering. For all the algorithms, the initial number of clusters was set to 40. The mean errors of the three approaches calculated for the entrance and T-intersection over different percentages of the overall trajectory length are plotted in Figure 7. It can be seen that the mean errors of the proposed approach are lower than those of the other two approaches in both scenes, which illustrate that the proposed approach can provide more accurate prediction results. Moreover, this error decreases steadily as more of the trajectory is observed, with the predictions made using 50% and 80% of the total trajectory producing mean errors of less than 1.3 and 1.0 m, respectively. This accuracy appears to be satisfactory for trajectory estimation with the objective of detecting traffic conflicts.

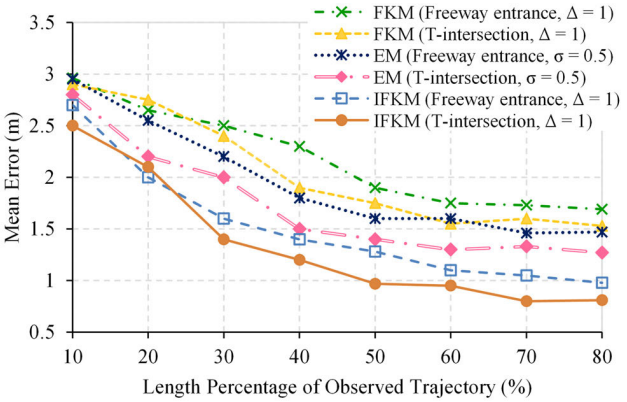

FIGURE 7. Mean error of trajectory estimation using different percentages of overall trajectory.

FIGURE 8. Test sequence of traffic conflict at freeway entrance.

FIGURE 9. Test sequence of traffic conflict at urban road T-intersection.

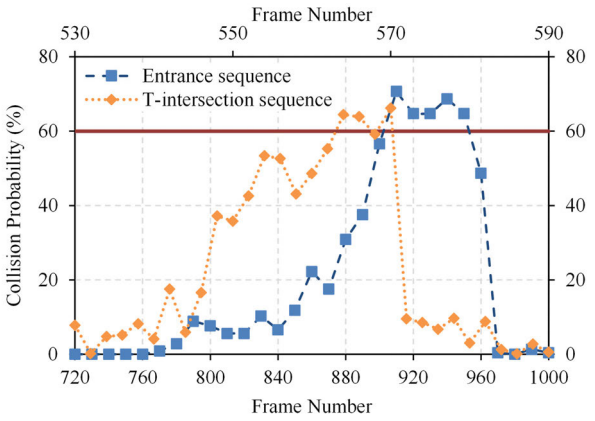

FIGURE 10. Collision probabilities of two manually identified traffic conflicts.

C. DETECTING TRAFFIC CONFLICTS WITH COLLISION ESTIMATION

Based on the trajectories predicted by the learned HMMs, the collision probabilities at different times of a developing interaction can be estimated using (21). Figures 8 and 9 show two manually identified traffic conflicts at the freeway entrance and T-intersection, respectively. In the entrance sequence, a truck first moves nearly parallel to a minivan and then accelerates to overtake it when gradually converging into the mainline. In this situation, the minivan driver does not initially adjust his or her driving, which leads to a rapid reduction in the distance between the two vehicles that exacerbates the conflict. Eventually, the driver has to decelerate to mitigate the high risk of collision. The calculated collision probability in this process, which is shown in Figure 10, begins at zero and then increases slightly but remains below 10% from frame 720 to frame 840. Thereafter, the probability begins to increase rapidly until it exceeds 60% at approximately frame 900. It remains at that level momentarily and finally decreases. In the T-intersection sequence, a car moving straight ahead approaches another one turning left as time goes on, with the degree of interference between the two increasing until the former has to decelerate to avoid collision. The collision probability corresponding to this process increases from 5.92% to 66.19% and thereafter sharply drops to 0, as shown in Figure 10.

From the two collision probability curves, it can be seen that the calculated results effectively reflect the ground truth of the corresponding vehicle interaction, suggesting that the proposed HMM-based algorithm for learning and predicting trajectories is suitable for collision probability calculation. The collision probability can be used as an indicator to reliably measure the degree of interference between vehicles. Furthermore, it is noteworthy that in terms of the high levels of collision probabilities in both the entrance and T-intersection sequences, conditions are undoubtedly created for easy identification of conflicts based on the severity indicator.

To further verify the effectiveness of the collision possibility calculated by the proposed method for traffic conflict detection, in addition to the two sequences analyzed earlier, an expanded experiment using entrance and T-intersection videos having durations of approximately 1 h each was performed. Tests were conducted on all interactions in which the vehicle separation became less than a specific distance. For each interaction, the collision probability between vehicles was calculated using the predicted trajectories. Then, an appropriate threshold was set to determine whether the interaction constituted a traffic conflict. To evaluate the effectiveness of the detection method, both videos were further analyzed by experienced observers, who determined that 81 and 107 traffic conflicts occurred at the entrance and T-intersection, respectively.

Table 2 lists the traffic conflict detection results obtained at the freeway entrance and T-intersection using different discriminant thresholds. It can be seen that, although the rate

TABLE 2. Traffic conflict detection results under different discriminant thresholds.

Threshold τ_P	Test scene	Number of conflicts detected manually	Traffic conflicts detected by the proposed method				
			Correct number	False number	Total number	Correct rate (%)	Success rate (%)
0.1	Entrance	81	79	70	149	53.02	97.53
	Intersection	107	103	67	170	60.59	96.26
0.3	Entrance	81	53	19	72	73.61	65.43
	Intersection	107	56	14	70	80.00	52.34
0.5	Entrance	81	14	3	17	82.35	17.28
	Intersection	107	21	2	23	91.30	19.63
0.7	Entrance	81	7	1	8	87.50	8.64
	Intersection	107	11	1	12	91.67	10.28

of correct traffic conflict detection increases steadily with the discriminant threshold, it does so at the expense of the success rate because the number of unidentified traffic conflicts increases simultaneously. This finding indicates that the discriminant threshold choice is crucial to both the quantity and quality of detected traffic conflicts. In this experiment, the most significant decrease in the success rate for the entrance occurs between $\tau_P = 0.3$ and $\tau_P = 0.5$, whereas the most significant growth in the correct rate occurs between $\tau_P = 0.1$ and $\tau_P = 0.3$, suggesting that a discriminant threshold (τ_P) of 0.3 is an appropriate tradeoff between completeness and practicality, because this value can identify at least 60% of conflicts while obtaining an correct rate of approximately 70%. Furthermore, in terms of the collision probability being an effective index for measuring the severity of a traffic conflict, selecting a higher threshold would be conducive to the identification of serious conflicts, which are the focus of road safety analyses. Accordingly, 0.1 appears to be a reasonable discriminant threshold for the T-intersection. Thus, by setting different discriminant thresholds for collision probability, the method proposed in this study can flexibly detect traffic conflicts while achieving results similar to those of human evaluations in terms of success rate.

IV. CONCLUSION

In this article, we presented a motion-pattern-based method of detecting traffic conflicts using trajectories extracted from video sensors. In particular, the generally overlooked usefulness of trajectories in characterizing motion was fully exploited using an original cluster-and-model algorithm. An improved fuzzy K-means algorithm that utilized the modified Hausdorff distance was proposed to cluster trajectories hierarchically based on their contained path and velocity information. By modeling the spatiotemporal characteristics of the trajectories in the obtained clusters, HMMs representing motion patterns were established and applied to predict trajectories having varying velocities as the weighted probability means of estimated states at different instances of time instead of the conventional distributions of all possible paths with respective constant velocities. Combining the prediction algorithm and the differences in terms of interaction safety under different *TTCs*, a probabilistic model for estimating collision probability was developed to detect traffic conflicts. The experimental results obtained using actual traffic video data indicated the feasibility and flexibility of the proposed method in identifying traffic conflicts from all vehicle interactions. The algorithm used for learning has advantages, such as avoiding the destructive pre-processing of trajectories, full usage of probabilistic approaches to model the spatiotemporal uncertainty of trajectories, and optimized targeting rather than absolute statistical predictions of trajectories covering velocity along with the development of traffic conflict.

Further, several limitations of this study should be noted. The proposed approach still relies on people to perform work in validating the trajectories and selecting the number of clusters, which to a certain extent restricts the degree of automation. Although the obtained results have proven the advantages of our algorithms, more experiments on different scenarios would be necessary to strengthen the conclusions. Future studies using historical crash data will also be required to validate the proposed traffic conflict detection approach further and to reveal the relationship between interactions with different collision probabilities and actual crash instances. A more challenging study would involve an exploration of how the proposed approach could be improved to allow for collision warnings between intelligent vehicles in actual traffic environments.

REFERENCES

[1] F. Amundson and C. Hydén, *Proceedings of the First Workshop on Traffic Conflicts*. Oslo, Norway: Institute of Transport Economics, 1977, pp. 1–6.

[2] G. R. Brown, "Traffic conflict for road user safety studies," *Can. J. Civ. Eng.*, vol. 21, no. 1, pp. 1–15, Feb. 1994.

[3] T. Sayed and S. Zein, "Traffic conflict standards for intersections," *Transp. Planning Technol.*, vol. 22, no. 4, pp. 309–323, Aug. 1999.

[4] C. Hydén, "The development of a method for traffic safety evaluation: The Swedish traffic conflict technique," Ph.D. dissertation, Dept. Traffic Plann. Eng., Lund Univ., Lund, Sweden, 1987.

[5] *Highway Safety Manual*, AASHTO, Washington, DC, USA, 2014, pp. 3–15.

[6] S. Atev, H. Arumugam, O. Masoud, R. Janardan, and N. P. Papanikolopoulos, "A vision-based approach to collision prediction at traffic intersections," *IEEE Trans. Intell. Transp. Syst.*, vol. 6, no. 4, pp. 416–423, Dec. 2005.

[7] A. Laureshyn, Å. Svensson, and C. Hydén, "Evaluation of traffic safety, based on micro-level behavioural data: Theoretical framework and first implementation," *Accident Anal. Prevention*, vol. 42, no. 6, pp. 1637–1646, Nov. 2010.

[8] P. St-Aubin, L. Miranda-Moreno, and N. Saunier, "An automated surrogate safety analysis at protected highway ramps using cross-sectional and before–after video data," *Transp. Res. C, Emerg. Technol.*, vol. 36, pp. 284–295, Nov. 2013.

[9] C. Wang, C. Xu, and Y. Dai, "A crash prediction method based on bivariate extreme value theory and video-based vehicle trajectory data," *Accident Anal. Prevention*, vol. 123, pp. 365–373, Feb. 2019.

[10] K. Xie, K. Ozbay, H. Yang, and C. Li, "Mining automatically extracted vehicle trajectory data for proactive safety analytics," *Transp. Res. C, Emerg. Technol.*, vol. 106, pp. 61–72, Sep. 2019.

[11] L. Xing, J. He, M. Abdel-Aty, Y. Wu, and J. Yuan, "Time-varying analysis of traffic conflicts at the upstream approach of toll plaza," *Accid. Anal. Prev.*, vol. 141, no. 1, pp. 1–14, Jun. 2020.

[12] S. M. S. Mahmud, L. Ferreira, M. S. Hoque, and A. Tavassoli, "Application of proximal surrogate indicators for safety evaluation: A review of recent developments and research needs," *IATSS Res.*, vol. 41, no. 4, pp. 153–163, Dec. 2017.

[13] W. Hu, X. Xiao, D. Xie, T. Tan, and S. Maybank, "Traffic accident prediction using 3-D model-based vehicle tracking," *IEEE Trans. Veh. Technol.*, vol. 53, no. 3, pp. 677–694, May 2004.

[14] N. Saunier and T. Sayed, "Probabilistic framework for the automated analysis of the exposure to road collision," *Transp. Res. Rec.*, vol. 2083, no. 1, pp. 96–104, Jan. 2008.
[15] C. Tay, "Analysis of dynamic scenes: Application to driving assistance," Ph.D. dissertation, Dept. Autom., Inst. Natl. Polytech. Grenoble, Grenoble, France, 2009.
[16] A. Tageldin, T. Sayed, K. Shaaban, and M. H. Zaki, "Automated analysis and validation of right-turn merging behavior," *J. Transp. Saf. Secur.*, vol. 7, no. 2, pp. 138–152, Apr. 2015.
[17] M. H. Zaki, T. Sayed, and S. E. Ibrahim, "Comprehensive safety diagnosis using automated video analysis: Applications to an urban intersection in edmonton, alberta, canada," *Transp. Res. Rec. J. Transp. Res. Board*, vol. 2601, no. 1, pp. 138–152, Jan. 2016.
[18] F. I. Bashir, A. A. Khokhar, and D. Schonfeld, "Object trajectory-based activity classification and recognition using hidden Markov models," *IEEE Trans. Image Process.*, vol. 16, no. 7, pp. 1912–1919, Jul. 2007.
[19] W. Hu, X. Xiao, Z. Fu, D. Xie, T. Tan, and S. Maybank, "A system for learning statistical motion patterns," *IEEE Trans. Pattern Anal. Mach. Intell.*, vol. 28, no. 9, pp. 1450–1464, Sep. 2006.
[20] D. Augustin, M. Hofmann, and U. Konigorski, "Prediction of highway lane changes based on prototype trajectories," *Forschung im Ingenieurwesen*, vol. 83, no. 2, pp. 149–161, Jul. 2019.
[21] D. Makris and T. Ellis, "Path detection in video surveillance," *Image Vis. Comput.*, vol. 20, no. 12, pp. 895–903, Oct. 2002.
[22] I. N. Junejo and H. Foroosh, "Trajectory rectification and path modeling for video surveillance," in *Proc. IEEE 11th Int. Conf. Comput. Vis.*, Rio de Janeiro, Brazil, 2007, pp. 1–7.
[23] D. Vasquez and T. Fraichard, "Motion prediction for moving objects: A statistical approach," in *Proc. IEEE Int. Conf. Robot. Autom. (ICRA)*, New Orleans, LA, USA, 2004, pp. 3931–3936.
[24] X. Wang, K. Tieu, and E. L. Grimson, "Learning semantic scene models by trajectory analysis," Dept. Comput. Sci. Artif. Intell. Lab., MIT, Cambridge, MA, USA, Tech. Rep. MIT-CSAIL-TR-2006-008, Feb. 2006.
[25] S. Atev, G. Miller, and N. P. Papanikolopoulos, "Clustering of vehicle trajectories," *IEEE Trans. Intell. Transp. Syst.*, vol. 11, no. 3, pp. 647–657, Sep. 2010.
[26] M. G. Mohamed and N. Saunier, "Behavior analysis using a multilevel motion pattern learning framework," *Transp. Res. Rec. J. Transp. Res. Board*, vol. 2528, no. 1, pp. 116–127, Jan. 2015.
[27] M. Bennewitz, W. Burgard, G. Cielniak, and S. Thrun, "Learning motion patterns of people for compliant robot motion," *Int. J. Robot. Res.*, vol. 24, no. 1, pp. 31–48, Jan. 2005.
[28] Q. Tran and J. Firl, "Online maneuver recognition and multimodal trajectory prediction for intersection assistance using non-parametric regression," in *Proc. IEEE Intell. Vehicles Symp.*, Dearborn, MI, USA, Jun. 2014, pp. 918–923.
[29] H. Jeong, Y. Yoo, K. M. Yi, and J. Y. Choi, "Two-stage online inference model for traffic pattern analysis and anomaly detection," *Mach. Vis. Appl.*, vol. 25, no. 6, pp. 1501–1517, Jul. 2014.
[30] D. Makris and T. Ellis, "Spatial and probabilistic modelling of pedestrian behavior," in *Proc. Brit. Mach. Vis. Conf.*, Cardiff, U.K., 2002, pp. 557–566.
[31] D. Vasquez, T. Fraichard, and C. Laugier, "Incremental learning of statistical motion patterns with growing hidden Markov models," *IEEE Trans. Intell. Transp. Syst.*, vol. 10, no. 3, pp. 403–416, Sep. 2009.
[32] N. Johnson and D. Hogg, "Learning the distribution of object trajectories for event recognition," *Image Vis. Comput.*, vol. 14, no. 8, pp. 609–615, Aug. 1996.
[33] N. Sumpter and A. Bulpitt, "Learning spatio-temporal patterns for predicting object behaviour," *Image Vis. Comput.*, vol. 18, no. 9, pp. 697–704, Jun. 2000.
[34] W. Hu, D. Xie, T. Tan, and J. Shen, "A hierarchical self-organizing approach for learning the patterns of motion trajectories," *Chin. J. Compu.*, vol. 26, no. 4, pp. 417–426, Apr. 2003.
[35] C.-E. Framing, F.-J. Heßeler, and D. Abel, "Learning scenario-specific vehicle motion models for intelligent infrastructure applications," *IFAC-PapersOnLine*, vol. 52, no. 8, pp. 111–117, 2019.
[36] L. Wang, L. Zhang, and Z. Yi, "Trajectory predictor by using recurrent neural networks in visual tracking," *IEEE Trans. Cybern.*, vol. 47, no. 10, pp. 3172–3183, Oct. 2017.
[37] M. Goldhammer, S. Köhler, S. Zernetsch, K. Doll, B. Sick, and K. Dietmayer, "Intentions of vulnerable road users-detection and forecasting by means of machine learning," *IEEE Trans. Intell. Transp. Syst.*, vol. 21, no. 7, pp. 3035–3045, Jul. 2020.
[38] C. Stauffer and W. E. L. Grimson, "Learning patterns of activity using real-time tracking," *IEEE Trans. Pattern Anal. Mach. Intell.*, vol. 22, no. 8, pp. 747–757, Aug. 2000.
[39] S. Kamijo, Y. Matsushita, K. Ikeuchi, and M. Sakauchi, "Traffic monitoring and accident detection at intersections," *IEEE Trans. Intell. Transp. Syst.*, vol. 1, no. 2, pp. 108–118, Jun. 2000.
[40] N. Saunier and T. Sayed, "Automated road safety analysis using video data," *Transp. Res. Rec.*, vol. 2019, no. 1, pp. 57–64, Jan. 2007.
[41] S. Lefèvre, D. Vasquez, and C. Laugier, "A survey on motion prediction and risk assessment for intelligent vehicles," *ROBOMECH J.*, vol. 1, no. 1, pp. 1–14, Jul. 2014.
[42] M. G. Mohamed and N. Saunier, "Motion prediction methods for surrogate safety analysis," *Transp. Res. Rec. J. Transp. Res. Board*, vol. 2386, no. 1, pp. 168–178, Jan. 2013.
[43] B. T. Morris and M. M. Trivedi, "Learning, modeling, and classification of vehicle track patterns from live video," *IEEE Trans. Intell. Transp. Syst.*, vol. 9, no. 3, pp. 425–437, Sep. 2008.
[44] B. T. Morris and M. M. Trivedi, "A survey of vision-based trajectory learning and analysis for surveillance," *IEEE Trans. Circuits Syst. Video Technol.*, vol. 18, no. 8, pp. 1114–1127, Aug. 2008.
[45] R. Xu and D. Wunsch, "Survey of clustering algorithms," *IEEE Trans. Neural Netw.*, vol. 16, no. 3, pp. 645–678, May 2005.
[46] L. Qu, F. Zhou, and Y. Chen, "Trajectory classification based on Hausdorff distance for visual surveillance system," *J. Jilin Univ.*, vol. 39, no. 6, pp. 1618–1624, Nov. 2009.
[47] B. Poritz, "Hidden Markov models: A guided tour," in *Proc. Int. Conf. Acoust., Speech, Signal Process.*, New York, NY, USA, 1988, pp. 7–13.
[48] L. R. Rabiner, "A tutorial on hidden Markov models and selected applications in speech recognition," *Proc. IEEE*, vol. 77, no. 2, pp. 257–286, Feb. 1989.
[49] A.-L. Bianne-Bernard, F. Menasri, R. A.-H. Mohamad, C. Mokbel, C. Kermorvant, and L. Likforman-Sulem, "Dynamic and contextual information in HMM modeling for handwritten word recognition," *IEEE Trans. Pattern Anal. Mach. Intell.*, vol. 33, no. 10, pp. 2066–2080, Oct. 2011.
[50] K. Tang, S. Zhu, Y. Xu, and F. Wang, "Modeling Drivers' dynamic decision-making behavior during the phase transition period: An analytical approach based on hidden Markov model theory," *IEEE Trans. Intell. Transp. Syst.*, vol. 17, no. 1, pp. 206–214, Jan. 2016.
[51] Å. Svensson, "A method for analysing the traffic process in a safety perspective," Ph.D. dissertation, Dept. Traffic Plann. Eng., Lund Univ., Lund, Sweden, 1998.
[52] G. A. Davis, J. Hourdos, H. Xiong, and I. Chatterjee, "Outline for a causal model of traffic licts and crashes," *Accident Anal. Prevention*, vol. 43, no. 6, pp. 1907–1919, Nov. 2011.
[53] Å. Svensson and C. Hydén, "Estimating the severity of safety related behaviour," *Accident Anal. Prevention*, vol. 38, no. 2, pp. 379–385, Mar. 2006.
[54] N. Lerner, "Age and driver perception-reaction time for sight distance design requirements," in *Proc. 65th Annu. Meeting Inst. Transp. Eng.*, Colorado, CO, USA, 1995, pp. 624–628.
[55] J. Wang, F. Zhang, and L. Zhang, "Halcon and OpenCV-based traffic automatic conflicting detecting method and data transaction," *J. Tongji Univ.*, vol. 38, no. 2, pp. 238–244, Feb. 2010.

ZONGYUAN SUN received the Ph.D. degree in road and railway engineering from Tongji University, Shanghai, China, in 2017. From 2009 to 2011, he was a Research Assistant with the Research Institute of Highway, Ministry of Transport, Beijing, China. Since 2018, he has been a Postdoctoral Research Fellow with the Department of Traffic and Transportation, Chongqing Jiaotong University, Chongqing, China. His research interests include traffic safety, visual surveillance, vehicle tracking, road user behavior, pattern recognition, and computer vision.

YUREN CHEN received the Ph.D. degree in road and railway engineering from Tongji University, Shanghai, China, in 1997. He is currently a Professor with the College of Transportation Engineering, Tongji University. His research interests include road environment and traffic conflict, video image processing, motion detection, machine learning, and computer-aided transportation engineering.

PIN WANG (Member, IEEE) received the Ph.D. degree in road and railway engineering from Tongji University, Shanghai, China, in 2016. From 2016 to 2017, she was a Postdoctoral Research Fellow with the Institute of Transportation Studies, University of California at Berkeley, Berkeley, CA, USA. Since 2017, she has been a Research Assistant with the California PATH, University of California at Berkeley. Her research interests include automated driving maneuvers, driving behavior, reinforcement learning, and motion planning.

SHOUEN FANG received the B.S., M.S., and Ph.D. degrees in road and transportation engineering from Tongji University, Shanghai, China, in 1984, 1994, and 2000, respectively.

In 1984, he joined the Department of Road and Transportation Engineering, Tongji University, where he first served as an Assistant Professor, then as an Associate Professor, and currently as a Professor. His research interests include road safety evaluation, traffic surveillance, traffic scene analysis, and collision warning systems.

BOMING TANG received the B.S. and Ph.D. degrees in road and transportation engineering from Southeast University, Nanjing, China, in 1985 and 1990, respectively.

He was a Postdoctoral Research Fellow and an Assistant Professor with Tongji University, from 1990 to 1992 and 1992 to 1995, respectively. In 1995, he joined the Nagaoka University of Technology, Niigata, Japan, as an Associate Professor with the School of Engineering. Since 2004, he has been a Professor with the Department of Traffic and Transportation, Chongqing Jiaotong University, Chongqing, China. His research interests include intelligent transportation systems, accident prevention, and statistical and stochastic modeling techniques. He is the Co-Chair of the Chinese Highway and Transportation Society.